Biochimica et Biophysica Acta, 1057 (1991) 399–406

ADONIS 000527289100116H

BBABIO 43367

Flash photolysis studies of manganese-depleted Photosystem II: evidence for binding of Mn^{2+} and other transition metal ions

Curtis W. Hoganson *, Patricia A. Casey and Örjan Hansson

Department of Biochemistry and Biophysics, Chalmers University of Technology and University of Göteborg, Göteborg (Sweden)

(Received 29 June 1990)
(Revised manuscript received 26 November 1990)

Key words: Photosystem II; Oxygen evolution; Manganese binding; Electron transfer kinetics; Flash absorption spectroscopy; $P680^+$ reduction kinetics

The reduction rate of $P680^+$, the oxidized form of the primary electron donor of Photosystem II, has been studied with flash absorption spectroscopy at 830 nm. Photosystem II membranes, partially depleted of the intrinsic manganese of the oxygen-evolving complex, were used. The reduction rate of $P680^+$ was measured as a function of the concentration of free Mn^{2+}, which was stabilized by metal-ion buffer systems consisting of chelators and metal-chelator complexes. Increasing the Mn^{2+} concentration induced an 18 to 35 μs decay component in the $P680^+$ reduction kinetics and diminished the amplitude of the 4 to 8 μs decay component. A dissociation constant of approx. 50 μM was obtained for the observed Mn^{2+} binding site. Other transition metal ions affected the reduction kinetics of $P680^+$ at lower concentrations. Thus, photooxidation of Mn^{2+} is not required for the detection of its binding at this site. To account for the kinetic effect, it is proposed that the bound metal ion interacts electrostatically with the tyrosine residue Y_Z, the intrinsic electron donor to $P680^+$.

Introduction

Electron transfer rates in proteins are sensitive to a number of parameters, one of which is the distribution of electrical charges near the reactants. Such charges alter the electron transfer rate by shifting the energy levels of reactants and of transition states. For example, in most reactions, one expects that a positive charge added near the electron donor will slow the reaction rate.

The presence of neighboring charges has been invoked to explain the different reaction rates that can be observed between two components of Photosystem II (PS II):

$$P680^+ + Y_Z \rightarrow P680 + Y_Z^+$$

where $P680^+$ (a chlorophyll species) is the oxidized form of the primary electron donor of PS II and Y_Z (a tyrosine residue of the D1 polypeptide) is the electron donor to $P680^+$. (For recent reviews on PS II structure and function see Refs. 1 and 2.) In both intact and deactivated PS II, an increase in positive charge near Y_Z apparently causes a decrease in the electron transfer rate. In intact PS II, possessing an active oxygen-evolving complex (OEC), the rate of this reaction depends on the S state of the OEC and becomes slower when positive charge is accumulated in the higher S states [3]. In PS II membranes in which the OEC has been destroyed chemically and its manganese atoms have been released, $P680^+$ is reduced by Y_Z with a halftime that increases from 2 to 20 μs upon lowering the pH from 8 to 5 [4]. This pH dependence has been attributed to the protonation of basic residues near Y_Z.

Abbreviations: DCBQ, 2,5-dichlorobenzoquinone; DCIP, 2,6-dichlorophenolindophenol; DPC, 1,5-diphenylcarbazide; NTA, nitrilotriacetic acid; OEC, oxygen-evolving complex; PS I, Photosystem I; PS II, Photosystem II; P680, the primary electron donor of PS II; Y_Z, a tyrosine residue of PS II.

* Present address: Department of Chemistry, Michigan State University, East Lansing, MI, U.S.A.

Correspondence: Ö. Hansson, Department of Biochemistry and Biophysics, Chalmers University of Technology and University of Göteborg, S-412 96 Göteborg, Sweden.

That manganese ions also bind to manganese-depleted PS II near Y_Z, is the conclusion of several analyses of the kinetics of electron flow through PS II. The photooxidation of H_2O_2 by PS II requires the presence of Mn^{2+}, which functions as an intermediate electron carrier [5–8]. Mn^{2+} has been shown to reduce the tyrosine radical Y_Z^+ directly [9]. Mn^{2+} also inhibits photooxidation of 1,5-diphenylcarbazide (DPC) by Y_Z^+ [10], although photooxidation of Mn^{2+} probably occurs during the inhibition. Further, the kinetics of photoactivation indicate a binding site for Mn^{2+} [11,12]. Estimated dissociation constants (actually inhibition constants or Michaelis constants) range from 0.04 μM to 50 μM.

The facts given above led us to predict that Mn^{2+}, when binding to manganese-depleted PS II membranes, would cause a decrease in the rate of reduction of $P680^+$ by Y_Z. In this paper, we report the results of experiments designed to test that prediction. Our results do indeed suggest binding of Mn^{2+} to manganese-depleted PS II and that this binding does slow the rate of electron transfer from Y_Z to $P680^+$, and further, that this effect does not depend on the photooxidizability of Mn^{2+}. We also suggest that a previously observed, minor phase in the $P680^+$ reduction kinetics, having a half-lifetime of 15 to 40 μs (Refs. 4, and 13–16 and references therein), is due to the presence of bound metal ions at a fraction of the PS II reaction centers. In addition, we compare the binding site identified here with the site(s) identified in other studies.

Materials and Methods

Sample preparation. PS II membranes were isolated from spinach [17,18]. Tris-washing was performed by incubating the membranes on ice in 0.8 M Tris-HCl (pH 8), 50 mM Na_2EDTA, for 20 min. The membranes were washed free of Tris and EDTA by centrifugation and resuspension three times in TMAHG buffer (20 mM tetramethylammonium hydroxide, 33% glycerol (v/v) and sufficient solid Hepes to obtain a pH 7.4). The membrane suspension (3 mg chlorophyll/ml) was frozen and stored in liquid nitrogen.

Manganese determinations of the membranes were performed using atomic absorption spectroscopy and the standard addition method, after incubation of the membranes with H_2SO_4. The Tris-washed membranes were found to contain approx. 1.4 Mn per P680, assuming 220 chlorophyll molecules per P680, while control membranes contained 4 Mn per P680.

Samples for kinetic analysis were prepared by adding to the measurement cuvette appropriate volumes of stock solutions to give 250 μM 2,5-dichlorobenzoquinone (DCBQ) (in dimethyl sulfoxide, final concentration 1%), 0.012% Triton X-100, chelator, $MnCl_2$ and Tris-washed PS II membranes (100 μg chlorophyll/ml) in TMAHG buffer. For all experiments except those shown in Fig. 2, the absorption transients produced by 40 flashes at 2 Hz repetition rate were averaged. Then 3 M KCl was added to give a final concentration of 50 mM, and further absorption transients were accumulated.

DCBQ was found to be a suitable redox mediator in that it completely reoxidized Q_A^-, the so-called primary acceptor of PS II, and completely reduced Y_Z^+ between flashes at a repetition rate of 2 Hz. This was determined by comparing the kinetic traces at flash repetition rates from 0.2 to 5 Hz. We found the amplitude of the absorption transient to be nearly independent of flash repetition rate, which indicates that Q_A^- is reoxidized between flashes. We also found that the lifetime of the absorption transient did not increase at higher flash repetition rates, which would have indicated that Y_Z^+ accumulated between flashes and that $P680^+$ was reduced by recombination with Q_A^- ($t_{1/2}$ = approx. 150 μs). Ferricyanide and phenyl-*p*-benzoquinone were tested but did not meet these criteria. Thus, in contrast to experiments using only ferricyanide as an electron mediator, we find very little 150 μs kinetics in our data [4,19]. Ferricyanide is unsuitable also because of the low solubility of the mixed potassium manganese ferrocyanide salts [20], particularly, $K_2Mn_3(Fe(CN)_6)_2$.

Mn^{2+} buffers. In order to know the concentration of free Mn^{2+} even at very low levels, we chose to buffer the Mn^{2+} concentration with Mn^{2+} and an excess of chelator. We used 1 mM of chelators and added from 100 μM to 900 μM $MnCl_2$ to stabilize the free Mn^{2+} concentrations at values between 10 pM and 500 μM. (The PS II reaction center concentration was approx. 0.5 μM.) The chelators used were EDTA, EGTA, nitrilotriacetic acid (NTA) and citrate. Others tried were 8-hydroxyquinoline sulfonate, oxalate and dipicolinic acid. The concentrations of free Mn^{2+} were calculated from the total Mn^{2+} concentration, total chelator concentration, pH and the equilibrium constants for the formation of the metal-chelator complex and protonation of the chelator. The equilibrium constants depend on the ionic strength of the solution. The appropriate values for citrate and NTA at the appropriate ionic strengths were calculated by a non-linear interpolation using tabulated data [21–23] and the following equation:

$$\log K(\mu) = \log K(0) - A \cdot f(\mu) \cdot (\delta Z^2)_{\text{eff}}$$

where $K(0)$ is the equilibrium constant at zero ionic strength, A is the Debye-Hückel constant (0.509 at 298 K) and $f(\mu)$ is the average of the ionic strength factors from the equations of Davies [24] and Scatchard [25] as given by Beck [26]. δZ^2 is the squared charge of the product ion minus the sum of the squared charges of the reactant ions. To ensure consistency with data in the

literature, $(\delta Z^2)_{eff}$ was calculated by applying the equation above to the tabulated data for 0 and 0.1 M ionic strengths. Table I indicates the values of the equilibrium constants used in and obtained from these calculations. Effects on these equilibrium constants due to the presence of 33% glycerol in our samples were neglected. The equilibrium constants for EDTA and EGTA were not corrected for ionic strength. In this paper, p*Mn* will be used as an abbreviation for $-\log_{10}([Mn^{2+}]/\text{molar})$.

Instrumentation and data treatment. Flash-induced absorption transients were measured at 830 nm with an apparatus essentially as described in Ref. 27 but with individual components as follows. The excitation pulse was from a frequency-doubled, Q-switched Nd:YAG laser (Quantel YG 571–10; wavelength, 532 nm; pulse duration, 10 ns). The pulse intensity, 1 mJ/cm^2 after attenuation with neutral density filters, nearly saturated the PS II signal. A temperature-stabilized diode laser (Melles Griot 06 DLD 003 driver and 06 DLL 503 head) provided a low-divergent (0.2 mrad) measuring light (25 mW at 830 nm) that passed through the cuvette (optical pathlengths: 10 and 4 mm for the measuring and excitation beams, respectively) onto an Si photodiode (UDT PIN-10D). An RG780 filter protected the photodiode from fluorescence and scattered light. The output from the photodiode was amplified with a home-built amplifier (gain, 50; bandwidth, 80 Hz to 30 MHz) and fed into an oscilloscope equipped with a multichannel plate cathode ray tube (Tektronix 11302A with 11A32 amplifier; bandwidth, 20 MHz). The oscilloscope trace was captured by a digitizing camera system (Tektronix DCS01) connected to a personal computer used for data treatment and storage. In all experiments, flash artifacts, obtained by blocking the measuring light, were subtracted from the transient absorbance signals. The measurements were performed at room temperature (20°C).

TABLE I

Equilibrium constants of Mn^{2+} chelators

Logarithms of the equilibrium constants at 298 K are presented. (a) Values taken from Refs. 21–23, (b) calculated values. n.a., not available; a value for log $K(0.15)$ of 3.54 [21] was used for the estimation of the citrate-Mn^{2+} equilibrium constants.

Chelator	Ion	Ionic strength (mol/l)			
		0 [a]	0.024 [b]	0.074 [b]	0.1 [a]
Citrate	H^+	6.39	5.99	5.77	5.70
Citrate	Mn^{2+}	n.a.	4.18	3.81	3.70
NTA	H^+	10.31	9.98	9.80	9.74
NTA	Mn^{2+}	8.59	7.89	7.52	7.40

Analysis of the kinetic traces in terms of a sum of two or three exponential decays together with a rising component to account for the limited time resolution of the setup were made with a nonlinear least-squares curve-fitting program based on the Levenberg-Marquardt algorithm [28].

Results

Tris-washed PS II membranes subjected to excitation by short flashes of light at 532 nm develop a transient absorbance at 830 nm due mainly to $P680^+$ (Fig. 1). The rise of the signal is instrument limited and its decay is pH dependent. The PS II inhibitor 3-(3,4-dichlorophenyl)-1,1-dimethylurea (DCMU) eliminates more than 90% of the signal in multiple flash experiments, including all of the fast phase, leaving only the slow phase due to Photosystem I ($P700^+$), whose true lifetime is obscured by the AC amplifier (approx. 2 ms time constant).

Addition of Mn^{2+} to Tris-washed PS II membranes increases the lifetime of the $P680^+$ signal to approx. 30 μs, while addition of EDTA decreases its lifetime to 7

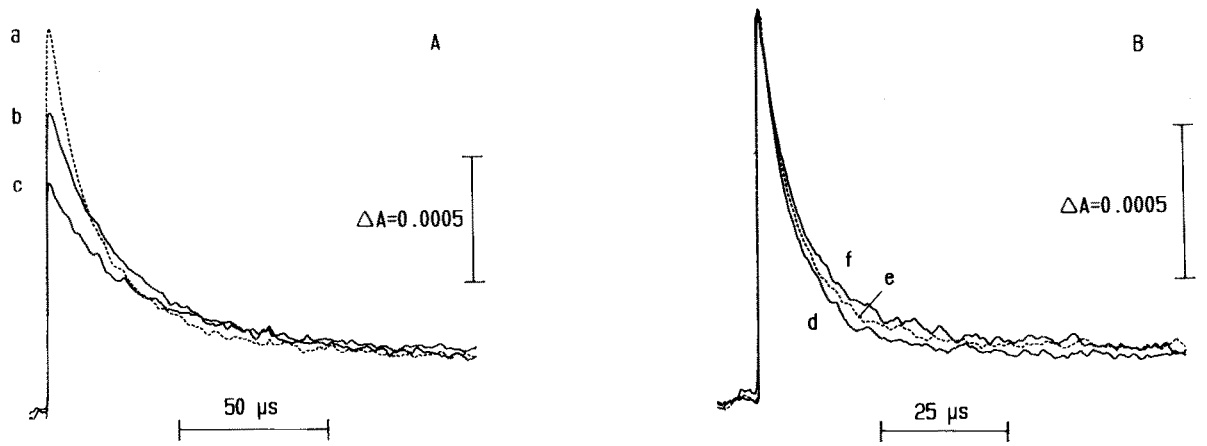

Fig. 1. Absorption transients at 830 nm of Tris-washed PS II membranes with added $MnCl_2$. Each sample contained PS II membranes (100 μg chlorophyll/ml), 250 μM DCBQ and 0.012% Triton X-100 in TMAHG buffer. (A) $MnCl_2$ was added to concentrations of (a) 31 μM, (b) 316 μM and (c) 1000 μM (p*Mn* 4.5, 3.5 and 3, respectively). (B) The concentration of free Mn^{2+} was stabilized with 1 mM NTA to (d) p*Mn* 6.3, (e) p*Mn* 5.3 and (f) p*Mn* 4.8.

μs. Membrane samples can be cycled repeatedly between excesses of Mn^{2+} or chelator and the kinetics of the $P680^+$ signal respond accordingly: thus, the effects of Mn^{2+} and EDTA are mutually reversible. EGTA and dipicolinic acid also promote fast kinetics, as does incubation of the membrane sample with chelating Sepharose (TM) followed by centrifugation, indicating that the effect is due to chelation of a metal ion rather than to a reaction of the chelators with the membranes (cf., Ref. 29). These chelator effects on the Tris- and EDTA-washed PS II membranes suggest that the washing procedure leaves some manganese ions (or other metal ions, see below) on the membranes, consistent with manganese determinations by atomic absorption which show 1.4 manganese atom per P680. Six micromolar EDTA was required to convert the $P680^+$ signal entirely to fast kinetics, probably by chelating Mn^{2+} or other metal ions (see below).

Concentrations of Mn^{2+} (or other divalent cations) above approx. 50 μM cause a decrease in the initial flash-induced absorbance change (Fig. 1A). The absorbance change remaining 200 μs after the flash is little affected. We attribute these observations to an increase in the stacking of the PS II membranes and the concomitant increase in their light scattering, which diminishes the extent to which they are detected in a transient absorption measurement. Membranes containing PS I are not prone to stacking and so the signal due to $P700^+$ is unchanged. This interpretation is consistent with a large body of observations of thylakoid membrane structure and dynamics, reviewed in Refs. 30 and 31.

The ionic strength of samples was increased by addition of 50 mM KCl. This also caused a decrease in the amplitude of the $P680^+$ signal, probably due to stacking of the PS II membranes. The rate of $P680^+$ reduction increased at higher ionic strength, as previously observed [4]. In some experiments, NaCl was added instead of KCl, producing similar results.

Careful examination of the traces in Fig. 1A shows that the lifetime of the signal due to $P680^+$ increases with the Mn^{2+} concentration. This phenomenon is seen also in Fig. 1B, which shows signals from samples buffered with NTA (p*Mn* from 6.3 to 4.8). In this concentration range, free Mn^{2+} does not induce noticeable membrane stacking, but it does alter $P680^+$ kinetics. Samples with EDTA (p*Mn* 11) or EGTA (p*Mn* 8.5) as the Mn^{2+} buffer gave signals essentially the same as those with NTA at a p*Mn* of 6.3.

We interpret these results to indicate that Mn^{2+} binds reversibly to a site near Y_Z and, by electrostatic forces, slows the rate of electron transfer from Y_Z to $P680^+$.

Control experiments to test whether Mn^{2+}-chelator complexes bind to the PS II membranes were performed by varying the total amount of chelator and Mn^{2+} added to the sample while keeping constant the calculated free Mn^{2+} concentration. For both citrate and NTA, whose complexes with Mn^{2+} are negatively charged, no significant differences in $P680^+$ kinetics were observed while varying the chelator concentration by a factor of ten. In contrast, experiments with the bidentate chelators oxalate and 8-hydroxyquinoline-5-sulfonate, which form neutral 1 : 1 metal-chelator complexes, suggest that these complexes do bind near Y_Z and retard $P680^+$ reduction. These observations are consistent with the negative surface charge at the PS II reaction center [4,32], which probably repels the anionic complexes.

Control experiments were also performed to test whether Mn^{3+} formed and persisted at the manganese binding site long enough to affect our measurements. The presence of Mn^{3+} at this binding site is expected to slow the Y_Z-$P680^+$ reaction rate more than Mn^{2+} does. By varying the flash repetition rate, from 2 Hz to 0.2 Hz, more time was allowed for reduction of Mn^{3+}, but we observed no change in the $P680^+$ signal (Fig. 2). The signal from $P700^+$ did increase in amplitude. This we attribute to more complete reduction of $P700^+$ between flashes. The large relative amplitude of $P700^+$ in these signals is due to scattering from stacked PS II membranes caused by the high Mn^{2+} concentration (p*Mn* 3.5) in this experiment. In other experiments, 250 μM hydroquinone or 400 μM H_2O_2 were added in order to increase the rate of reduction of Mn^{3+}, but in neither case did the $P680^+$ lifetime change. With H_2O_2, a smaller $P680^+$ signal was observed, probably due to a decreased concentration of exogenous electron acceptor. We conclude that in our samples, the observed PS II photochemistry lasts less than the half-second between flashes and that the effects we observe are due to Mn^{2+} and not to Mn^{3+}.

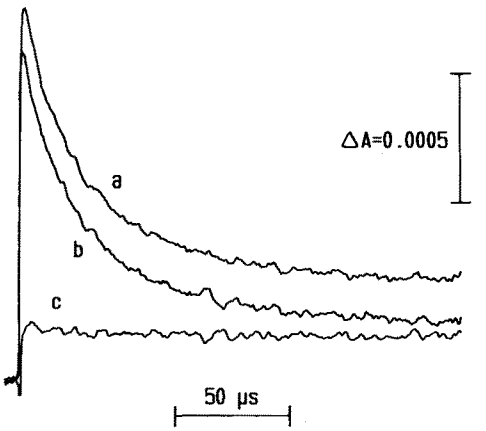

Fig. 2. Absorption transients at 830 nm of Tris-washed PS II membranes at two flash repetition rates. The sample contained 316 μM $MnCl_2$ and other contents as in Fig. 1A. The averages of 30 transients are shown; ten transients were collected at 2 Hz, then ten at 0.2 Hz, then ten at 2 Hz, etc. (a) 0.2 Hz, (b) 2 Hz and (c) the arithmetic difference between traces a and b.

To obtain more detailed information about the $P680^+$ kinetics, the absorption transients were analyzed with a computer program which calculates the sum of exponential decay functions best fitting the experimental data. The kinetics are interpreted in terms of the following model.

In any sample, the PS II reaction centers can be divided into two populations, those with Mn^{2+} bound near Y_Z and those without Mn^{2+} bound, and each population has its characteristic electron-transfer rate constant. If the binding and release of Mn^{2+} are slow compared with the electron transfer, then the two populations of reaction centers will not be in equilibrium during the measurement, and two separate kinetic phases will be observed. However, if the binding and release of Mn^{2+} are fast compared with the electron transfer, then the two populations will be in equilibrium and will give rise to a single decay component – such behavior would be analogous with the pH effect on $P680^+$ reduction kinetics [4]. In addition, a slow component is needed to describe the PS I signal. Therefore, either two or three exponential decay functions were used in the data analysis.

For samples with low values of free Mn^{2+} ($pMn > 5$), the traces were well fit by a sum of two exponentials. The faster phase, whose lifetime depends on ionic strength and pH, as described by Conjeaud and Mathis [4], accounts for 90% of the initial amplitude of the transient. Its 1/e lifetime was 7.4 and 3.6 μs at ionic strengths of 24 and 74 mM, respectively. It represents the reduction of $P680^+$ by Y_Z in reaction centers where Mn^{2+} is not bound.

At higher concentrations of free Mn^{2+}, the traces required the sum of three exponentials for a good fit (Fig. 3). For these data sets, the lifetime of the fastest component was fixed at the value obtained from samples with low Mn^{2+} concentrations and the lifetime of the slowest phase was fixed at the 2 ms amplifier limit. The amplitudes of all three components were allowed to vary freely. The lifetime of the intermediate phase determined by this fitting procedure was found to be approx. 28 and 18 μs at 24 mM and 74 mM ionic strengths, respectively, with a slight tendency towards higher values at higher Mn^{2+} concentrations. We believe that this intermediate phase represents reaction centers where Mn^{2+} is bound at the time of the flash. Because biphasic reduction of $P680^+$ is observed, we conclude that the binding and release of Mn^{2+} from the reaction center are not fast compared with the electron transfer from Y_Z to $P680^+$.

To compare the populations of PS II with and without bound Mn^{2+}, we used the initial amplitudes of the two kinetic phases of $P680^+$ (obtained from the fitting procedure) and calculated the fraction in the fastest phase (Fig. 4). When this fraction equals 0.5, the two populations are equal and the concentration of Mn^{2+} equals

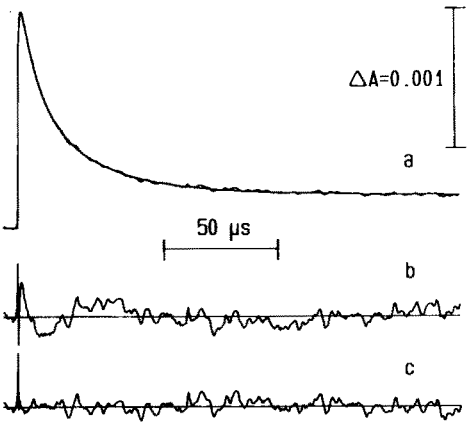

Fig. 3. Absorption transient and curve-fitting analysis of the data. The sample contained 31 μM $MnCl_2$ as in Fig. 1A, trace a. (a) The result of a three decay component fit is plotted together with the experimental data. (b) Residuals plot of a two-component fit: the difference between the experimental data and the fitted data is shown. Both amplitudes and both lifetimes were fitted. A worse fit was obtained if the longer lifetime was fixed at 2 ms. (c) Residuals plot of the three component fit shown in a: the lifetimes of the fastest and slowest components were fixed at 7.4 μs and 2 ms, respectively. All three amplitudes and the intermediate lifetime were fitted. An additional rising component (time constant, 0.65 μs) was included in both fits to account for the limited time resolution of the apparatus. The residuals were magnified five times before plotting.

the dissociation constant for Mn^{2+} at this site. The dissociation constant is thus approx. 40 μM at 24 mM ionic strength. At 74 mM ionic strength, a value of approx. 55 μM was obtained.

To characterize further this Mn^{2+} binding site, we tested its ability to bind other metal ions. In experiments analogous to those described above, but without the use of metal ion buffers, we added divalent ions Ca^{2+}, Mg^{2+}, Co^{2+}, Ni^{2+}, Cu^{2+} and Zn^{2+}. Neither Ca^{2+} (up to 1.5 mM) nor Mg^{2+} slow $P680^+$ kinetics, nor do they diminish the effect induced by the presence of Mn^{2+}, although they do induce stacking of the membrane fragments. In contrast, Co^{2+}, Ni^{2+}, Cu^{2+} and

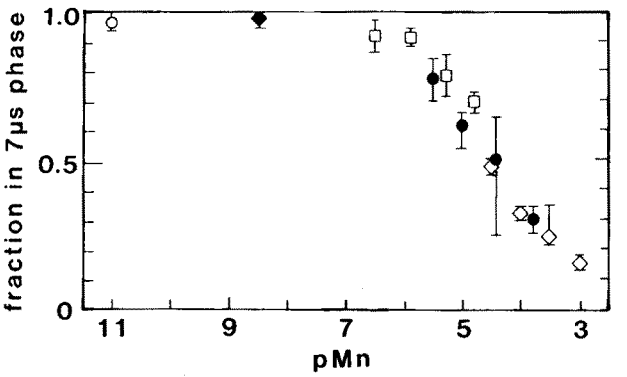

Fig. 4. Dependence on the free Mn^{2+} concentration of the fraction of PS II showing 7.4 μs kinetics. The ionic strength was 24 mM. The manganese buffers used were EDTA (○), EGTA (◆), NTA (□), citrate (●) and none (◇). Other contents of the samples were as in Fig. 1.

Zn^{2+} do slow $P680^+$ reduction very markedly (Fig. 5). The effects saturate at 10 μM or less, so the dissociation constants must be smaller than 10 μM. Because these dissociation constants are lower than that observed for Mn^{2+}, binding can be observed without the complication of membrane stacking and the concomitant increased light scattering: the initial amplitude of the $P680^+$ signal is not altered by adding a concentration of metal ion sufficient to saturate the effect on the kinetics. Furthermore, since these ions are not oxidized by PS II, the redox state of the DCBQ pool is not altered by their addition so that the signal amplitude from $P700^+$ is not altered either. These results therefore greatly strengthen our interpretation of the results obtained with Mn^{2+}. In particular, they show that the effect we have observed is not a secondary effect either of the ability of Mn^{2+} to be oxidized by PS II or of its ability to induce membrane stacking of the membrane fragments, but is independent of both phenomena.

The $P680^+$ kinetics in the presence of saturating Ni^{2+}, Cu^{2+} or Zn^{2+} are slowed to approx. 70 μs (1/e lifetime). There is some preliminary evidence that at subsaturating concentrations, the $P680^+$ decay has 1/e phases of both 22 μs and 70 μs. Thus, it may be that two ions may bind near Y_Z and influence the Y_Z-$P680^+$ electron transfer rate.

From the above results, the metal ion specificity of this binding site follows the usual pattern for polydentate chelators containing multiple carboxylate groups where K_{diss} for the several ions are ordered: Mg^{2+}, $Ca^{2+} > Mn^{2+} > Co^{2+}$, Ni^{2+}, Cu^{2+}, Zn^{2+}.

Mn^{2+} is a competitive inhibitor of DPC photooxidation by PS II [10]. The observed K_M for DPC is 150 μM. In order to compare the binding site observed here with that seen in the DPC-DCIP assay, we added DPC to a final concentration of 300 μM to a PS II membrane sample containing 100 μM Mn^{2+} and 250 μM DCIP.

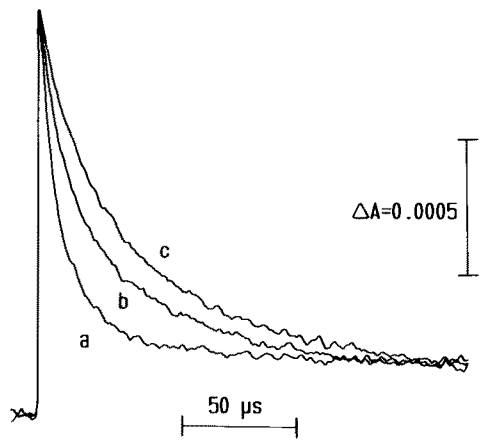

Fig. 5. Absorption transients at 830 nm of Tris-washed PS II membranes in the presence of $CuCl_2$. 250 μM DCBQ, 0.012% Triton X-100 and 6 μM EDTA were present. (a) 0, (b) 3.3 and (c) 6.7 μM $CuCl_2$.

This produced no change in the $P680^+$ reduction kinetics. Therefore, DPC and Mn^{2+} do not seem to compete for binding at the site described here. The ability of DPC to form complexes with the transition metal ions Ni^{2+}, Cu^{2+} and Zn^{2+} precluded their use in analogous competitive binding studies.

Discussion

In this paper the rate of the Y_Z to $P680^+$ electron transfer reaction in Tris-washed PS II membranes was studied as a function of added transition metal ion concentration. Evidence was presented that these ions bind to a site on PS II from which they retard the electron transfer from Y_Z to $P680^+$, perhaps by electrostatic interactions. Because manganese is a component of the OEC, most experiments involved addition of Mn^{2+}, but qualitatively similar results were obtained with four other transition metal ions. Thus, in contrast with previous reports of reactions of Mn^{2+} with PS II [5–12], the effects we observe here do not involve oxidation of the Mn^{2+}. Release of Mn^{2+} from this binding site is slow compared to the electron transfer rate so that distinct kinetic decay phases occur which correspond to PS II either with or without Mn^{2+} bound.

Minor kinetic components of $P680^+$ decay in the range of 15 to 40 μs have been observed previously in thylakoid or PS II membranes that were Tris-washed or otherwise inhibited (Refs. 4,13,14,16 and references therein). Our results suggest that these kinetic components may be induced by the presence of bound metal ions. Because the dissociation constants for some of the transition metal ions is rather low, the binding site is sensitive to contaminants from buffers or metal ions released from the decomposition of other metalloproteins in the sample.

The appearance of a kinetic component with a 35 μs half-lifetime was also noted in oxygen-evolving PS II membranes, and its amplitude was found to be S-state dependent [15]. We suggest that the apparent S-state dependence may be an artifact of the limited bandwidth of the amplifier used and of the fitting procedure, which assumed there to be no flash number dependence of the other microsecond decay components. As the total amplitude of the microsecond components of $P680^+$ decay was less than 15% of the total $P680^+$ signal, with the rest decaying in less than 1 μs, it is reasonable to attribute the 35 μs component to centers inactive in oxygen evolution.

The presence of these kinetic phases in experiments performed in many laboratories underscores the need, at times, for careful control of trace metal ion concentrations and the general nature of this problem. Our results (see Fig. 4) show that chelators can sometimes be used to provide a wide, if not continuous, range of well-defined concentrations of free metal ions. Using

several chelators, we were able to stabilize the free Mn^{2+} concentration over a p*Mn* range of 6.5, which facilitated detection of binding of Mn^{2+} to Tris-washed PS II. However, to prevent undesired interferences, some care must be exercised in the choice of chelator. For example, we found that the metal-chelator complexes of oxalate and 8-hydroxyquinoline-5-sulfonate with Mn^{2+} also retarded the $P680^+$ reduction kinetics.

The Mn^{2+} binding site that we have identified resembles that deduced from studies of photoactivation kinetics [11,12]. Ono and Inoue found dissociation constants of 40 μM for Mn^{2+} and of greater than 3 mM for Ca^{2+}, and Miller and Brudvig calculated dissociation constants of 51 ± 5 μM for Mn^{2+} and of 70 ± 40 mM for Ca^{2+} for a site involved in the rate-limiting step in photoactivation. These numbers are similar to those we obtained from $P680^+$ kinetics. We suggest that the photoactivation experiments and our measurements identify the same binding site and that it is one of the manganese binding sites of the OEC.

In contrast, the sites for Mn^{2+} detected by the H_2O_2-DCIP assay [5–8], by the DPC-DCIP assay [10] and by time-resolved EPR measurements of the Y_Z^+ lifetime [9] have much lower K_M values (K_I in the case of DPC-DCIP), between 0.04–1 μM for Mn^{2+}. In both the H_2O_2-DCIP assay and in the time-resolved EPR measurements, Ca^{2+} and Mg^{2+} were found to inhibit the reactions with inhibition constants of approx. 0.3 to 1 mM. This inhibition may operate simply by lowering the surface potential, which decreases the surface concentration of Mn^{2+}, rather than by direct binding of the competing ion at the binding site. The DPC-DCIP reaction was inhibited much less by Co^{2+} and Zn^{2+} than by Mn^{2+} and even less by Ca^{2+} and Mg^{2+}. The addition of NaCl weakened the inhibition by Mn^{2+}, indicating a surface potential effect.

Because of the strength of Mn^{2+} binding at these sites, they appear to be distinct from the site that we have identified. There then would be two classes of manganese in the OEC, as indicated by the nature of their binding sites. This is consistent with the many reports that chelators easily remove not all four but two of the manganese atoms (e.g., Refs. 33,34), but it is possible that the manganese atoms not readily extractable by chelators are in higher oxidation states than II.

It is curious that the tightly binding Mn^{2+} produces no perturbation of the Y_Z-$P680^+$ reaction rate; Mn^{2+} bound to these sites reacts rapidly with Y_Z^+ so these sites must be rather near Y_Z. As the measurements which show submicromolar dissociation constants for manganese involve oxidation of Mn^{2+} to Mn^{3+}, the Michaelis or inhibition constants determined thereby may not be the true dissociation constants for Mn^{2+}. This might account for their absence from our flash experiments. On the other hand, it is reasonable to think that the rate of photoactivation would be limited by the binding of Mn^{2+} to the lowest affinity site, so the high-affinity sites may well be real. Furthermore, the transitions of the OEC from S_0 to S_1 and from S_2 to S_3 produce rather little change in the Y_Z-$P680^+$ reaction rate, while the S_1 to S_2 transition produces a measureable change in that reaction rate [3,35]. Thus, it appears that oxidation of manganese at certain of these sites, whether because of geometry or distance or compensating charge displacements, produces little effect on the Y_Z-$P680^+$ reaction rate, and these factors may also determine whether binding of Mn^{2+} exerts an effect on $P680^+$ reduction kinetics. It would, however, be premature to identify the site of the manganese ion oxidized on the S_1 to S_2 transition with the site of the manganese ion whose binding we report here.

The existence of a metal binding site with higher affinity for Cu^{2+} than for Mn^{2+} suggests that Cu^{2+} may inhibit photosynthetic oxygen evolution by replacing Mn^{2+}. In studies using Hepes buffer (pH 7.5) and DCIP as an electron acceptor, values for K_I of 5 μM [36] and 8 μM [37] were determined. These inhibition constants agree well with the binding of Cu^{2+} that we observed.

Although much remains to be worked out concerning the nature of manganese binding to PS II, we have identified a means of detecting the presence of Mn^{2+} at what may be one of the native binding sites of the OEC. This technique, in combination with chemical modification of amino acid residues or site-directed mutagenesis, should be useful when searching for possible ligands to the manganese atoms involved in photosynthetic oxygen evolution.

Acknowledgements

We thank Professor Tore Vänngård and Dr. Lars-Erik Andréasson for helpful discussions. This work was supported by the Knut and Alice Wallenberg Foundation (purchase of the laser) and the Swedish Natural Science Research Council.

References

1 Babcock, G.T., Barry, B.A., Debus, R.J., Hoganson, C.W., Atamian, M., McIntosh, L., Sithole, I. and Yocum, C.F. (1989) Biochemistry 28, 9557–9565.
2 Hansson, Ö. and Wydrzynski, T. (1990) Photosynth. Res. 23, 131–162.
3 Brettel, K., Schlodder, E. and Witt, H.T. (1984) Biochim. Biophys. Acta 766, 403–415.
4 Conjeaud, H. and Mathis, P. (1986) Biophys. J. 49, 1215–1221.
5 Velthuys, B. (1983) in The Oxygen Evolving System of Photosynthesis (Inoue, Y., Crofts, A., Govindjee, Murata, N., Renger, G. and Satoh, K., eds.), pp. 83–90, Academic Press, Tokyo.
6 Boussac, A., Picaud, M. and Etienne, A.-L. (1986) Photobiochem. Photobiophys. 10, 201–211.
7 Inoue, H. and Wada, T. (1987) Plant Cell Physiol. 28, 767–773.

8 Inoue, H., Akahori, H. and Noguchi, M. (1987) Plant Cell Physiol. 28, 1339–1343.
9 Hoganson, C.W., Ghanotakis, D.F., Babcock, G.T. and Yocum, C.F. (1989) Photosynth. Res. 22, 285–293.
10 Hsu, D.-B., Lee, J.-Y. and Pan, R.-L. (1987) Biochim. Biophys. Acta 890, 89–96.
11 Ono, T.-A. and Inoue, Y. (1983) Biochim. Biophys. Acta 723, 191–201.
12 Miller, A.-F. and Brudvig, G.W. (1989) Biochemistry 28, 8181–8190.
13 Eckert, H.-J., Renger, G. and Witt, H.T. (1984) FEBS Lett. 167, 316–320.
14 Van Gorkom, H.J. (1985) Photosynth. Res. 6, 97–112.
15 Schlodder, E., Brettel, K. and Witt, H.T. (1985) Biochim. Biophys. Acta 808, 123–131.
16 Schlodder, E. and Meyer, B. (1987) Biochim. Biophys. Acta 890, 23–31.
17 Berthold, D., Babcock, G.T. and Yocum, C.F. (1981) FEBS Lett. 134, 231–234.
18 Ghanotakis, D.F., Babcock, G.T. and Yocum, C.F. (1984) Biochim. Biophys. Acta 765, 388–398.
19 Gerken, S., Dekker, J.P., Schlodder, E. and Witt, H.T. (1989) Biochim. Biophys. Acta 977, 52–61.
20 Bellomo, A., De Marco, D. and Casale, A. (1972) Talanta 19, 1236–1240.
21 Sillén, L.-G. and Martell, A.E. (compilers) (1964) Stability Constants of Metal-Ion Complexes, The Chemical Society, London, Burlington House.
22 Sillén, L.-G. and Martell, A.E. (compilers) (1971) Stability Constants of Metal-Ion Complexes, The Chemical Society, London, Burlington House, Supplement No. 1.
23 Perrin, D.D. (compiler) (1979) Stability Constants of Metal-Ion Complexes: Part B: Organic Ligands, IUPAC Chemical Data Series-No. 22, Pergamon Press, Oxford.
24 Davies, C.W. (1938) J. Chem. Soc. 2093.
25 Scatchard, G. (1936) Chem. Rev. 19, 309.
26 Beck, M.T. (1970) Chemistry of Complex Equilibria, p. 28, Van Nostrand Reinhold, London.
27 Van Best, J. and Mathis, P. (1978) Biochim. Biophys. Acta 503, 178–188.
28 Press, W.H., Flannery, B.P., Teukolsky, S.A. and Vetterling, W.T. (1988) Numerical Recipes in C. The Art of Scientific Computing, pp. 540–547, Cambridge University Press, Cambridge.
29 Wydrzynski, T. and Renger, G. (1986) Biochim. Biophys. Acta 851, 65–74.
30 Anderson, J.M. (1984) in Advances in Photosynthesis Research (Sybesma, C., ed.), Vol. 3, pp. 1–10, Martinus Nijhoff, The Hague.
31 Barber, J. (1984) in Advances in Photosynthesis Research (Sybesma, C., ed.), pp. 91–98, Martinus Nijhoff, The Hague.
32 Yerkes, C.T. and Babcock, G.T. (1981) Biochim. Biophys. Acta 634, 19–29.
33 Packham, N.K. and Barber, J. (1984) Biochim. Biophys. Acta 764, 17–23.
34 Satoh, K. and Katoh, S. (1985) Biochim. Biophys. Acta 806, 221–229.
35 Bouges-Bocquet, B. (1980) Biochim. Biophys. Acta 594, 85–103.
36 Samuelsson, G. and Öquist, G. (1980) Plant Cell Physiol. 21, 445–454.
37 Renganathan, M. and Salil, B. (1990) Photosynth. Res. 23, 95–99.